**Research Article**

# Dealing with Non-orthogonally Measured Telluric Components in Magnetotellurics

**Ji-yang Kim, Gang-sop Kim[*] and Yong-kil Kim**

Faculty of earth science and technology, Kimchaek University of Technology, Republic of Korea

**[*]Corresponding Author**

Gang-sop Kim, Faculty of earth science and technology, Kimchaek University of Technology, Republic of Korea, Email: kgs6673@star-co.net.kp

**Abstract**

In Magnetotellurics, two telluric and three magnetic components of the magnetotelluric field are generally recorded at the ground in the Cartesian coordinate system. In practice, however, there are some difficult cases for setting two telluric- lines orthogonally to record telluric components due to obstacles like roads, wetlands, rivers, cliffs, rice banks, buildings, etc. at a given MT site.

In this paper, we propose a method of converting telluric components recorded in non-orthogonal coordinate systems to those in orthogonal coordinate systems by means of mathematical coordinate transformation and verify its possibility and applicability through model and field tests. Probably, this method should be of great interest to MT field crews for freely choosing site position and set electric lines.

**Keywords:** Magnetotellurics, Data Processing, Non-Orthogonal Coordinate System

## Introduction

Magnetotellurics (MT) is a deep electromagnetic exploration method to study subsurface resistivity structures from tens to hundreds of kilometers depth using natural electromagnetic field of the earth caused by solar wind and lightning activity [1,2]. After the first study in 1953 [3], many variants such as tensor method [4], audio frequency MT [5], radiofrequency MT [6], marine MT [7], are developed and widely used in different problems, including groundwater [8], geothermal [9,10], metal [11], petroleum [7,12], and etc.

In general, the MT records the time series of two telluric and three magnetic components of the electromagnetic(EM) field at the surface in orthogonal coordinate system with x, y, and z axes, oriented in the north, east and vertical directions, respectively. Therefore, two dipoles consisting of a pair of nonpolar electrodes (called commonly telluric or electric lines, briefly E-lines) should be installed to measure the telluric field. The

E-lines can be in the form of + or L shape and its length is 50–200 m. The longer the length, the better the signal-to-noise ratio, but the effect of AC voltage on the local power network can be increased.

At stations where the E-lines cannot be inevitably set in the north-south and east-west direction, the observation coordinate system is generally rotated. However, in this case, the E-lines should be orthogonal to each other [13]. For example, the EMSLAB data [14] were recorded with an x-axis in the magnetic north direction of -19.5° declination. Also, the SAMTEX data [15,16] were collected with different azimuth angle of the x-axis which is generally not a true north direction.

However, in reality, there are difficult cases to orthogonally install two E-lines, due to the local surface conditions such as roads, wetlands, rivers, cliffs, rice banks, buildings, etc. In such case, it may be a solution to make the dipole length longer, but this is not a good way in viewing working efficiency. Alternatively, one can inevitably move the site position, but it is also not a good way, since the exploration design has been already given.

An example is shown in Figure 1. As shown in this figure, it is difficult to set the E- lines orthogonally at stations 1-1 and 3-1 located at the corner of the island, because of the river flowing. Such situations are frequently encountered in mountainous, forest and urban areas, too.

In this paper, we propose a method to convert the MT telluric data measured at non-orthogonal setup of E-lines into those in orthogonal coordinate system by mathematical coordinate transformation and show the model and field tests.
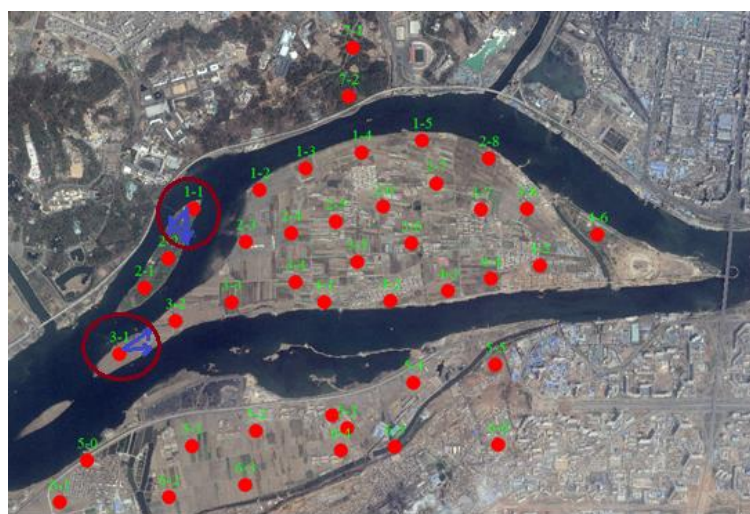


**Figure 1:** Example of sites that is difficult to set the E-lines at right angles (perpendicular) in MT (Duru Island region in Pyongyang; number-site label, red circle-site. It is really impossible to set the E- lines orthogonally at the sites 1-1, 3-1, etc.)

## Method

We assume that the telluric components are measured in the non-orthogonal coordinate system with the x'-axis deviated by angle α from the north direction (x-axis) and the y'-axis deviated by angle β from the east direction ( y-axis ) (Figure 2). So, the problem is to determine the telluric components Ex and Ey in the Cartesian coordinate system xoy from the actually measured telluric components $E_{x'}$ and $E_{y'}$ which are ne-

cessary for data processing [17-19]. Here, we note that this problem can be derived in both time and frequency domains and angle α is generally not equal to β. Actually, the interconversion of a vector quantity between different coordinate systems is also discussed in the branch of precision mechanisms [20].

In Figure 2, the vectors $E_{x'}$ and $E_{y'}$, are the projections of telluric field vector **E** to x' and y' axes, respectively. Thus, vectors $E_{x'}$ and $E_{y'}$ are represented by $E_x$ and $E_Y$ as follows:

$$E_{x'} = E_x \cos\alpha + E_y \sin\alpha$$
$$E_{y'} = -E_x \sin\beta + E_y \cos\beta \qquad (1)$$

Rewriting Eq. 1 into a matrix form gives

$$\begin{pmatrix} E_{x'} \\ E_{y'} \end{pmatrix} = \begin{pmatrix} cos\alpha & sin\alpha \\ -sin\beta & cos\beta \end{pmatrix} \begin{pmatrix} E_x \\ E_y \end{pmatrix} \qquad (2)$$

From Eq.(2), we can obtain Eq.(3).

$$\begin{pmatrix} E_x \\ E_y \end{pmatrix} = \begin{pmatrix} \cos\alpha & \sin\alpha \\ -\sin\beta & \cos\beta \end{pmatrix}^{-1} \begin{pmatrix} E_{x'} \\ E_{y'} \end{pmatrix}$$

$$\begin{pmatrix} E_x \\ E_y \end{pmatrix} = \frac{1}{\cos(\alpha - \beta)} \begin{pmatrix} cos\beta & -sin\alpha \\ sin\beta & cos\alpha \end{pmatrix} \begin{pmatrix} E_{x'} \\ E_{y'} \end{pmatrix} \qquad (3)$$

By Eq. (3), we can find the vector components $E_x$ and $E_y$ in the Cartesian coordinate system xoy from components $E_{x'}$ and $E_{y'}$ and angles α and β. That is, the telluric components observed in the non-orthogonal coordinate system (x'oy') can be mapped to those in the orthogonal coordinate system (xoy). Reversely, by Eq. (1), the telluric components in the orthogonal coordinate system may be mapped to the non-orthogonal coordinate system, too.

## Synthetic Example

Mathematically, Eqs. 2 and 3 are strictly derived transformation formulas. However, it is necessary to validate in MT, whether it is actually effective to convert the MT data observed in non-orthogonal coordinate system into the orthogonal coordinate system, via the model calculation.

First, we generate the synthetic MT signal. To this end, some methods are available [21-23]. Among those, we use the method of [23].
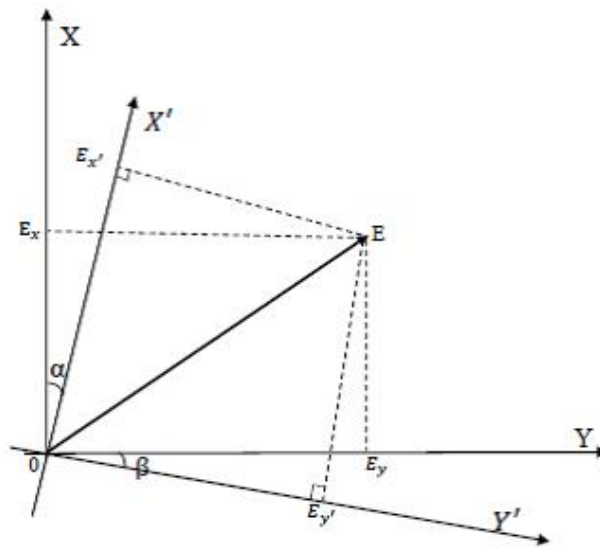
**Figure 2:** Geometry of MT telluric field vector in orthogonal and non-orthogonal coordinate systems (xoy-orthogonal coordinate system, x'oy'- non-orthogonal coordinate system, **E**-telluric field vector, Ex, Ey - x and y components of E, respectively, $E_{x'}, E_{y'}$ – x' and y' components of E, respectively, α, β - angles between x and x' axes and between y and y' axes, respectively).

The sampling frequency and the length of the time series are chosen as fs = 150 Hz (Δt = 6.6667 ms), and N = 16384. The frequency number of the signal is N/2 in the interval [fs/N, fs/2] and the mutually independent complex white noise spectrum s = ($s_x$, $s_y$) is generated as follows:

$$s_x = n_x^{w,real} + i \cdot n_x^{w,imag}, s_y = n_y^{w,real} + i \cdot n_y^{w,imag} \quad (4)$$

The impedance Z(f) is simply calculated for a three-layered medium with resistivity $\rho_{xy}$ = [1000, 100, 1000] Ωm, $\rho_{yx}$ = [1000, 100, 1000]/2 Ωm, and thickness h = [1000, 500]m.

Then, the MT spectra are calculated as follows:

$$E = s \cdot Z^{1/2}, H = s \cdot inv\left(Z^{1/2}\right) \quad (5)$$

Through inverse Fourier transform of the above spectra, we can get the synthetic MT time series.

Figure 3 shows the resulted time series of two horizontal components as solid lines. The dotted line in the figure is the transformation of the simulated signal to the measured signal in a non-orthogonal coordinate system with α=10º, β=-20º according to Eq. (3);

while the black points show the reconstructed time series from the non-orthogonal coordinate systems to the original orthogonal coordinate system using Eq.(2). Fig. 3 (b) shows the zooming of the [0, 1]s interval.

Figure 4 shows the hodograph of the telluric vector in the Cartesian coordinate system, where (a) is the whole signal and (b) is the [0, 1] seconds interval.

Here, we can intuitively see that the original synthetic signal is mapped to a non-orthogonal coordinate system and then converted back to the orthogonal coordinate system, the accurate reconstruction is made.

In conclusion, we find that the vector field measured in the non-orthogonal coordinate system can be reproduced in the orthogonal coordinate system without ambiguity, provided that the measuring noise is not considered.
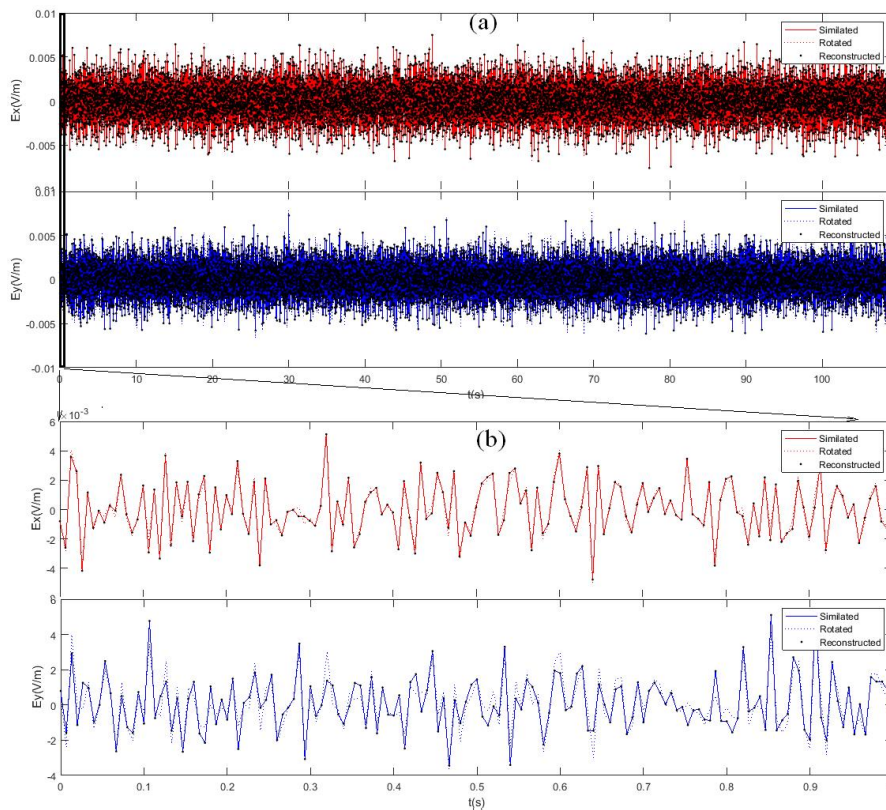
**Figure 3:** Time series of simulated telluric time series(solid line) and corresponding time series in non-orthogonal coordinate system with **α=10°, β=-20°** (dotted line) and reconstructed it to the original coordinate system (dot) (a) total data, (b) 0-1 second interval.
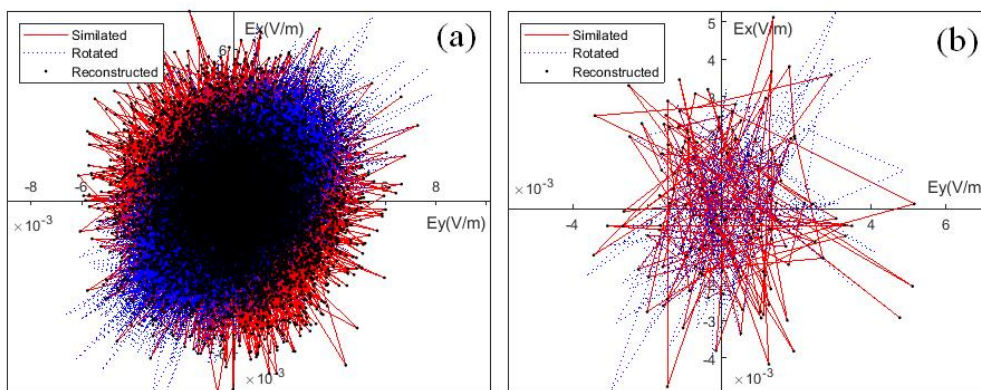


**Figure 4:** Time series of simulated telluric field time series(solid line) and corresponding time series in non-orthogonal coordinate system with **α=10°, β=-20°** (dotted line) and reconstructed it to the original coordinate system (dot) (a) total data, (b) 0-1 second interval.

**Field Test**

In order to verify the validity of the proposed method, we carried out a test measurement at a MT site (05-01 (39°49'19″N, 124°13'59″E)) in the northwest of the Korean peninsula. As mentioned in [24], this site is at a rural area more than 20 km from nearby city, where it is possible to measure relatively high quality data.

We acquired MT data using a 5-channel receiver, three magnetic induction sensors, and two electrical dipoles with Pb-P-bCl$_2$ electrodes, manufactured in Kim Chaek University of Technology (KUT). The sampling frequency of the three sub-bands are fs = 2400 Hz, 150 Hz and 15 Hz ($\Delta$t = 4.166667x10-4 s, 6.666667x10-3 s, 6.666667x10-2 s).

First, both the magnetic and telluric sensors were installed in the correct north-south and east-west directions to make the data observation (orthogonal observation).

Next, only the E-lines were artificially installed in the directions of $\alpha$ = 10$°$ and $\beta$ = -20$°$, respectively to make the data observation (non-orthogonal observation).

The number of recording samples is N = 327680 for each sub-band, respectively, and the data recording time for orthogonal and non-orthogonal observations is about 6 h, respectively.

The MatLab code [24] was used for the recorded MT data processing.

Figure 5(a) shows the sounding curves obtained from the processing of orthogonal observation data. As shown in the figure, curves are relatively consistent with those of [24].

Next, the processing results of non-orthogonal observations are shown in Figure 5(b).

As shown in the figure, since the actual non-orthogonal observations are assumed to be orthogonal, the results are quite different from those obtained with orthogonal conditions (Figure 5(a)). In particular, the $\rho$xy curve corresponding to the off-diagonal impedance is shifted upward and $\rho$yx curve is shifted downward, especially the displacement of the $p_{yx}$ curve is larger. This can be related to the fact of $\alpha = 10°, \beta = -20°, |\alpha| < |\beta|$.

Then, the non-orthogonal observations were transformed by the proposed method, mapped to the observations of the orthogonal conditions, the resulted curves are shown in Figure 5(c). As shown in the figure, almost similar results are obtained with the realistic orthogonal observation (Figure 5a). The difference is somewhat large in the low frequency part, which may be related to the measuring noise.

It is important to conclude that even when the E- lines are installed up non-orthogonally, the proposed method enable to obtain curves similar to the orthogonal setup by simple coordinate transform.
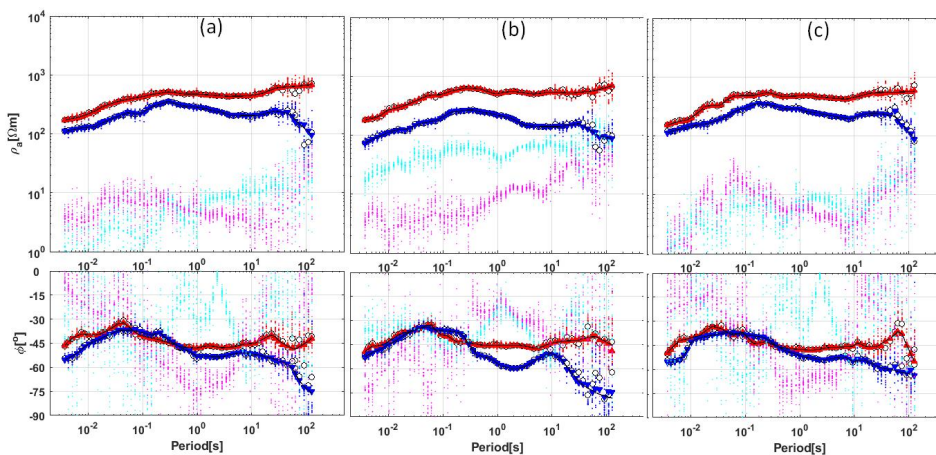


**Figure 5:** Field test of the proposed method at site 5-1 (39°49'19″N, 124°13'59″E).

(a), (b) are curves for orthogonal and non-orthogonal data, respectively; (c) is for orthogonal data converted from the non-orthogonal observations by the proposed method; the upper and lower panels in a, b, c correspond to apparent resistivity and phase curves; red, blue, magenta, and cyan colored denote the xy, yx, xx and yy components, respectively.

## Discussion and Conclusion

We have studied a simple method to deal with the data, which are inevitably measured using non-orthogonal E-lines at a given site, due to local surface conditions in MT. The mutual transformation formulae between orthogonal and non-orthogonal observations are derived, coded, and validated by synthetic calculation and tested at a MT site with low noise. The examples clearly show that close agreement can be achieved with realistic orthogonal observation and reconstructed one from non-orthogonal observations. Hence, we conclude as follows.

- When inevitably not installed E- lines at right angles, one can convert the measured non-orthogonal data into the orthogonal data by the proposed method.

- What is more important is that using this method, E-lines can be installed in arbitrary convenient orientation. However, the actual orientation angles of the E- lines must be measured accurately.

In fact, the application of MT has been considerably limited due to the increased noise level and the difficulty in choosing sites as urbanization progresses [25,26]. For example, [26] noted that Urbanization is a biggest challenge nowadays for the application of MT as it introduces cultural noises and results in the limited availability of locations for the data acquisition. Therefore, using this method, MT field crews can achieve considerable convenience in choosing site location and E- line set-up.

Further work is needed to test this method at other MT sites and to extend the applicability of the method based on more rigorous simulation of MT time series data in complex 3D media.

## Acknowledgement

## Data Availability

All the data needed to draw the conclusions of this paper will be stored in the Kim Chaek University of Technology (www.kut.edu.kp) or other reliable data warehouse and will be downloaded and publicly available after receipt of the manuscript.

The request before that must be addressed to the contact author.

## References

1. Berdichevshy MN (1968) Electrical prospecting with magnetotelluric profiling, Nedra, Moscow.

2. Simpson F, Bahr K (2005) Practical Magnetotellurics, Cambridge University Press.

3. Cagniard L (1953) Basic theory of the magneto-telluric method of geophysical prospecting, Geophysics, 18: 605-35.

4. Swift CM (1967) A magnetotelluric investigation of an electrical conductivity anomaly in the southwestern United States, PhD thesis, MIT, Boston, MA.

5. Garcia X, Jones AG (2008) Robust processing of magnetotelluric data in the AMT dead band using the continuous wavelet transform. Geophysics, 73: F223-34.

6. Tezkan B, Georgescu P, Fauzi U (2005) A radiomagnetotelluric survey on an oil-contaminated area near the Brazi Refinery, Romania, Geophysical Prospecting, 53: 311-23,

7. Meju MA, Saleh AS (2023) Using Large-Size Three-Dimensional Marine Electromagnetic Data for the Efficient Combined Investigation of Natural Hydrogen and Hydrocarbon Gas Reservoirs: A Geologically Consistent and Process-Oriented Approach with Implications for Carbon Footprint Reduction, Minerals, 13: 745.

8. Yusuf SN, Wamtas IG, Imagbe LO, Yohanna OM (2022) 2D magnetotelluric inversion of basement complex rocks of Tangur for groundwater exploration, North Central Nigeria, SCIENCE FORUM (Journal of Pure and Applied Sciences) 22: 541-9.

9. Zhang L, Hao T, Xiao Q, Wang J, Zhou L, et al. (2015) Magnetotelluric investigation of the geothermal anomaly in Hailin, Mudanjiang, northeastern China, Journal of Applied Geophysics, 118: 47-65.

10. Cheng Yuanzhi, Wang Cheng, Da Wenwei, Kong Yanlong, Hu Xiangyun (2023) Anatomy of the convective geothermal system from geophysical and hydrochemical data: A case study from the Changshou geothermal field, South China, GEOPHYSICS, 88: WB1-10.

11. Comeau MJ, Becken M, Kuvshinov AV, Demberel S (2021) Crustal architecture of a metallogenic belt and ophiolite belt:implications for mineral genesis and emplacement from 3-D electrical resistivity models (Bayankhongor area, Mongolia), Earth, Planets and Space, 73: 82

12. Christopherson KR (1991) Applications of magnetotellurics to petroleum explorationin PapuaNew Guinea: A model for frontier areas, Geophysics:The Leading Edge of Exploration, 21-7.

13. Phoenix Geophysics (2005) System 2000.net User Guide, chapter 12. Magnetotellurics (MT) and Audiofrequency MT (AMT), 231-91

14. Wannamaker PE, Booker JR, Filloux JH, Jones AG, Jiracek GR, et al. (1989) Magnetotelluric observations across the Juan de Fuca subduction system in the EMSLAB project. Journal of Geophysical Research, 94: 111-14.

15. Jones AG, RL Evans, MR Muller, MP Hamilton, MP Miensopust, et al. (2009) Area selection for diamonds using magnetotellurics: Examples from southern Africa. Lithos, 112S: 83-92.

16. Khoza D, Jones AG, Muller MR, Evans RL, Webb SJ, Miensopust M, (2013) the SAMTEX team, 2013. Tectonic model of the Limpopo belt. Precambrian Res. 226: 143-56.

17. Chave AD, Thomson DJ (2004) Bounded influence magnetotelluric response function estimation, Geophys. J. Int., 157: 988-1006

18. Egbert GD, Livelybrook DW, (1996) Single station magnetotelluric impedance estimation: Coherence weighting and the regression M-estimate, Geophysics, 61: 964-70

19. Weckmann U, Magunia A, Ritter O (2005) Effective noise separation for magnetotelluric single site data processing using a frequency domain selection scheme. Geophys. J. Int. 161: 635-52.

20. Fern Florian, Füßl Roland, Eichfelder Gabriele, Manske Eberhard, Kühnel Michael (2021) Coordinate transformation and its uncertainty under consideration of a non-orthogonal coordinate base, Measurement Science and Technology. 32: 045001.

21. Varentsov IM, Sokolova E Yu (1995) Generation of synthetic magnetotelluric data, PHYSICS OF THE SOLID EARTH, English Translation, 30: 6.

22. Loddo M, Schiavone D, Siniscalchi A, (2002) Generation of synthetic wide-band electromagnetic time series, ANNALS OF Geophysics, 45: 289-301

23. Neukirch, M., Garcia, X., 2014.Nonstationary magnetotelluric data processing with instantaneous parameter. J. Geophys. Res. Solid Earth 119, 1634–1654

24. Kim Gang-Sop, Cho Gyong-Rae, Kang Jong-Nam, Pak Yong-Chol, Ri Sung-Hyon, Hu Xiang-Yun, (2018) Constrained smoothness optimization of bootstrapped transfer functions for handling noisy MT data, Journal of Applied Geophysics, 155: 226-31.

25. Li G, Zhou X, Chen C, Xu L, Zhou F, Shi F, Tang J, (2023) Multitype Geomagnetic Noise Removal via an Improved U-Net Deep Learning Network, IEEE TRANSACTIONS ON GEOSCIENCE AND REMOTE SENSING, 61: 5916512

26. Ajithabh KS, Patro PK, (2023) SigMT: An open-source Python package for magnetotelluric data processing, Computers & Geosciences, 171: 105270.

**CEOS Publishers** follow strict ethical standards for publication to ensure high quality scientific studies, credit for the research participants. Any ethical issues will be scrutinized carefully to maintain the integrity of literature.

## Publication Ethics

## Plagiarism Policy

## Copyrights

**CEOS Publishers** believes scientific integrity and intellectual honesty are essential in all scholarly work. As an upcoming publisher, our commitment is to protect the integrity of the scholarly publications, for which we take the necessary steps in all aspects of publishing ethics.

All the articles published in **CEOS Publisher** journals are licensed under Creative CommonsCC BY 4.0 license, means anyone can use, read and dow-nload the article for free. However, the authors reserve the copyright for the published manuscript.